Vortex-Induced Vibrations for Energy Harvesting: A Review

G. K. Chhaparwal and Ram Dayal

1 Introduction

The rise of hunger for energy demand is inevitable but the adverse environmental effects of carbon emission by burning of fossils to meet this demand can be avoided. Paris Agreement in 2015 further motivated researchers and investors around the globe to see future in carbon-free renewable energy resources. The rise in worldwide capacity of solar energy and wind energy in last five years also shows that the time when renewable energy will be major source of energy is no more distant. But in this paper, a new type of technique is reviewed that exploits ocean energy in an entirely different way—VIVACE (vortex induced vibration for aquatic clean energy) which is invented by Bernitsas in 2004–05 [1–5]. Before moving to what is VIVACE, let us discuss why do we need VIVACE? The habitat coastal areas have very high real estate property values, and surrounding marine life and environment further make such areas not friendly with other renewable energy options like solar power plant and wind turbines. Many countries have made very strict rules that must be satisfied by the any device that could be installed in these areas. Those are low maintenance, high life, robustness, high energy density, and should not obstruct navigation. There were many other ocean energy harvesting-based devices but all failed to meet the standards required to be installed along the coastal areas like water column, buoy, flap, pendulum [6, 7], turbines, watermills [8, 9], etc.

G. K. Chhaparwal
Rajasthan Institute of Engineering and Technology, Jaipur, Rajasthan 302026, India

R. Dayal (✉)
Department of Mechanical Engineering, Malaviya National Institute of Technology Jaipur, Jaipur, Rajasthan 302017, India
e-mail: ramdayal.mech@mnit.ac.in

D. Sharma and S. Roy (eds.), *Emerging Trends in Energy Conversion and Thermo-Fluid Systems*, Lecture Notes in Mechanical Engineering,
https://doi.org/10.1007/978-981-19-3410-0_22

1.1 Ocean Energy

The ocean is full of different types of energy that can be harnessed to fulfill the ever growing demand of the global energy consumption specially, along the coastal areas where the cost of land and existing flora and fauna are also major concern. For a sustainable energy harvesting, an energy convertor must follow certain criteria as shown in Fig. 1 (Table 1).

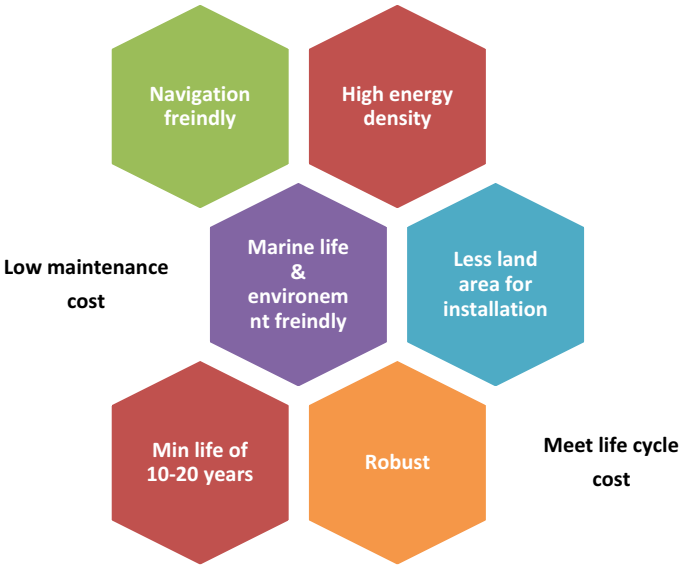

Fig. 1 Minimum criteria required by an ocean energy convertor for a sustainable energy harvesting

Table 1 Various conventional ocean energy convertors and their limitations

Convertor of	Limitations
Surface oscillation (water column, buoy, flap, or pendulum)	High energy output only near resonance, random waves hardly attain optimal performance with often extreme structural loads
Wind and tidal energy (turbines and watermills)	Low efficiency and inefficient function below 2 m/s (~4 knots), disturb marine life and occupy expensive coastal area for operation
Potential energy (water dams)	High water head requirement, large in structure, obtrusive, significant capital cost and construction period, and disturb marine life

1.2 Vortex-Induced Vibrations

In *VIVACE* which is a type of an ocean energy convertor, the suspended circular bars or cylinders are fixed on a vertical column via elastic springs of sufficiently high stiffness. The reciprocating motion (up and down) of the cylinders is synchronized and finally converted into the rotary motion via rack and pinion gear system to get electricity through a generator arm. The fundamental understanding of vortex-induced vibrations (*VIV)* is prerequisite before learning the working of *VIVACE.* The free and forced vibrations of such fixed rigid structures with single or multiple *dof* (degrees of freedom) lay the foundation of principle working of *VIVACE* device. The cylinders oscillate transverse to the velocity of water with weak in-line and strong transverse nonlinear oscillations [10].

The lock-in stage is very important in the vortex-induced vibrations. It is also known as vortex synchronization. At this stage, $f_{\text{form}} \sim f_{\text{n,water}} \sim f_{\text{cyl}}$ or simply the vortex formation and natural frequencies both become almost equal to each other. The unique construction characteristic of the *VIVACE* device allows the synchronization to happen over a larger range of reduced velocity and at high mass ratio as compared to the other convertors. Where reduced velocity factor $U^* = \frac{U}{f_{\text{n, water}} D}$ and mass ratio $m^* = \frac{m_{\text{osc}}}{m_{\text{d}}}$ and $m_{\text{d}} = \frac{\pi}{4} \rho_{\text{w}} D^2 L$ [11–14].

It can be observed that there are many ways to harness energy from ocean, but it was Bernitas and his team who successfully exploited vortex had induced vibration (*VIV*) first time for feasible and sustainable energy harvesting through their invented device called VIVACE in year 2004–05. Unlike other ocean energy-based devices, it is safe for marine life. It is based on the *VIV.* The *VIV* involves several degrees of freedom, and it is self-induced and self-limiting with several mode of responses. Reynolds number (Re) and damping (C) have unusually very high values, which have limited studies in the literature. There are many parameters whose effect can be investigated as briefly discussed in the following points in Table 2.

In a study by [5], the effect of high damping, high Re, and variable R_{L} (for optimization of the electricity generated) is investigated in a Low-Turbulence Free-Surface Water (*LTFSW*) channel with all the necessary mathematical.

2 Experimental Model

2.1 LTFSW *Channel*

The *LTFSW* channel has many advantages over a towing tank which is used to get flow past a cylinder. It provides unlimited number of oscillations per experiment within acceptable turbulence level. However, in *LTFSW,* the width of the channel limits the length of the cylinder and turbulence induced by impeller makes it difficult to achieve very low turbulence level. A two-story high water channel recirculates

Table 2 Table captions should be placed above the tables

Parameter	Explanation
Synchronization or lock-in	It depends on mass ratio which changes the wake pattern properties
Range of synchronization about natural frequency of the cylinder	A broad range of synchronization in VIV makes the device robust against the changes in the flow velocity
Self-limiting amplitude	A suitably high magnitude of the VIV oscillation is managed through energy harnessing resistance which should not suppress VIV oscillation
Initial, upper, and lower branches of amplitude of oscillation	A VIVACE device must work in high damping and high amplitude for wide range of synchronization
Types of wake pattern (2S, 2P, P + S, 2 T)	It depends on the values of mass ratio (m^*) and degree of freedom
Mass ratio (m*):	It is ratio of oscillating mass to the displaced fluid mass which changes types of response and vibrational frequency
Multiple degrees of freedom	A two degree of freedom causes higher amplitudes of the oscillation
Correlation length	It is ratio of the length to the diameter of the cylinder; its larger value is preferred for higher forces on the cylinders
Synchronization under high damping	A less work is reported in literature on this parameter, and higher damping is maintained that can sustain VIV
Reynolds number	The amplitude of oscillation and lift increase with Re, and it is also less investigated in the literature
Proximity to the free surface or solid boundaries	Wake structure and forces on cylinder significantly change with the closeness of the surface of fluid or solid
Product ($m^*\zeta_a$)	A sustainable large *VIV* oscillation amplitude must be maintained to get maximum possible power generation. An optimum trade-off between high damping and generated power obtained so that too much damping should not suppress *VIV*

8000 gallons of treated water via four impeller of diameter 0.787 m connected with 20 hp three-phase electric motor.

2.2 Apparatus

Figure 2 shows the *VIVACE* cylinder placed transverse to the fluid flow as a spring-mass system with all dimensions, stiffness, and damping in the setup. Initially, three setup *VIVACE* models were studied, out of which Model-III works in the desired

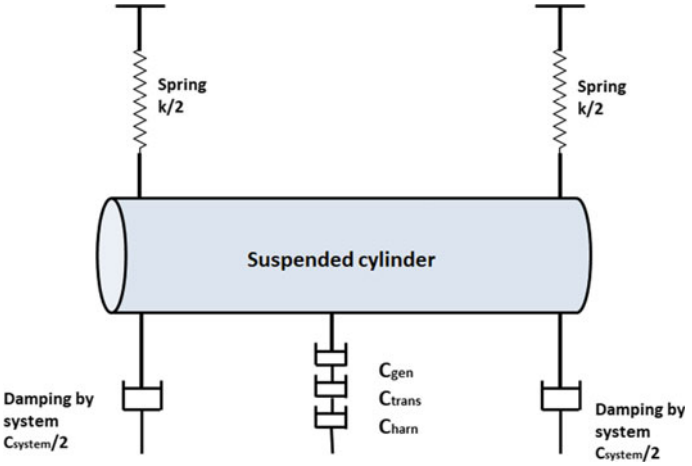

Fig. 2 *VIVACE* cylinder placed transverse to the fluid flow as a spring-mass system

manner. The cylinder in the Model-III is made up of aluminum, and it has diameter $D = 125.7$ mm, length $L = 914.4$ mm, aspect ratio $L/D = 7.274$, and a high blockage ratio $D/H = 0.143$. There are two cylinders with a gap of 10 mm with the walls of the test section, which are suspended by compression coil springs at the ends, with constrained motion in transverse direction via linear bearings and controlled natural frequency of oscillation $f_{\text{n,water}}$ (0.88–1.037 Hz) via changing the active coils.

2.3 Calibration

The velocity measured from the pitot tube placed 30 cm from bottom of the tank and half-width of the tank is calibrated with the velocity of the *VIVACE* cylinder at six water depths with four impeller frequencies within range of velocity 1.2 m/s (above this value, there was non-uniformity in the correlation) for 30 s of time period, and a correlation is developed as given by:

$$U\,(\text{m/s}) = (-0.000034 \times (\text{ Water Depth(cm)}) + 0.061177) \times \text{ Impeller Frequency} \quad (1)$$

The input from transducer and generator is fed into the data acquisition system. The amplitude and range of synchronization are significantly reduced as cylinder is placed closer to the free surface.

3 Mathematical Modeling

Equation of motion for the *VIVACE* cylinder,

$$(m_{\text{osc}} + C_{\text{a}})\left[\frac{y^*}{f_{\text{n, water}}^2} + \frac{4\pi\zeta_{\text{total}}y^*}{f_{\text{n, water}}} + 4\pi^2 y^*\right] = \frac{2}{\pi}c_y(t)U^{*2} \tag{2}$$

Fluid power in VIVACE

$$P_{\text{VIVACE, fluid}} = \frac{1}{2}\rho\pi c_y U^2 f_{\text{cyl}} y_{\max} DL \sin(\varphi) \tag{3}$$

Mechanical power in VIVACE,

$$P_{\text{VIVACE, fluid}} = 8\pi^3(\text{mosc} + \text{Ca})\zeta_{\text{total}}\left(f_{\text{cyl}}y_{\max}\right)^2 f_{\text{n, water}} \tag{4}$$

Upper limit to the efficiency of the *VIVACE* converter (based on the experimental data):

$$\eta_{\text{UL, VIVACE}} = \frac{P_{\text{VIVACE, fluid}}}{P_{\text{fluid}}} \tag{5}$$

where power in fluid is given by $1/2\rho U^3 DL$; the efficiency of the *VIVACE* device is given by:

$$\eta_{\text{VIVACE}} = \frac{P_{\text{VIVACE, harn}}}{P_{\text{fluid}}} \tag{6}$$

Generator Model

Torque generated in the generator is given by (Fig. 3):

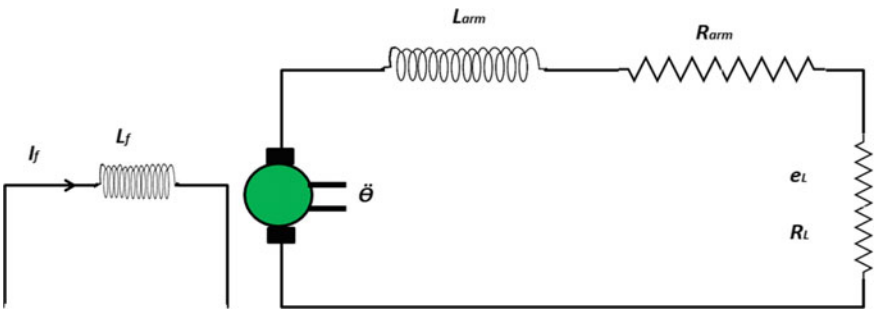

Fig. 3 An equivalent electric circuit diagram of a VIVACE device

$$T_{\text{gen}} = (k_{\text{f}} I_{\text{f}})\left(\overline{k} I_{\text{arm}}\right) = K I_{\text{arm}} \tag{7}$$

The voltage generator by field induced by the VIV is given by:

$$\frac{\tilde{\theta}}{\tilde{e}_{\text{L}}} = \frac{-K}{\omega^2 \text{JL}_{\text{arm}} + i\omega(L_{\text{arm}} c + R_{\text{arm}} J) + R_{\text{arm}} c - \alpha K} i\omega \tag{8}$$

Transmission Model

The periodic reciprocating (up and down) motion of the cylinder is converted into the periodic rotational oscillatory motion of the shaft of the generator with the help of a rack and pinion gear system, which is shown in Fig. 4. When the gear effect is considered, the expression for the voltage-induced can be written as:

$$\frac{\tilde{\theta}}{\tilde{e}_L} = \frac{-K}{\omega^2 J L_{eq} + i\omega\left(L_{arm} c_1^{eq} + R_{arm} J_1^{eq}\right) + R_{arm} c - \alpha K} i\omega$$

Combined Model

Here, all the components of the *VIV and* energy generation via transmission systems are combined together to get an overall view of the interlinking of the individual system. Due to inertia of the movement of the generator, gear-2 exerts force on the suspended cylinder. There are frictional losses in the gear system as well as damping in the generator due to electric wiring. Both can be managed by the L_{R}(load resistor). All kinds of the damping can be put together to get an interrelationship via following equation:

$$C_{\text{total}} = C_{\text{system}} + C_{\text{trans}} + C_{\text{gen}} + C_{\text{harn}} \tag{10}$$

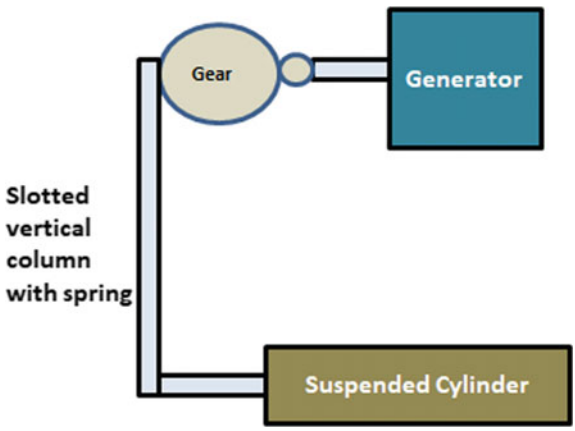

Fig. 4 A schematic diagram showing all the components of a VIVACE device [5]

Table 3 Different types of damping in the *VIVACE* and their causes

Damping	Cause	Measurement
System damping, C_{system}	It is due to structural damping by friction at the component and the material scales and fluid damping which is the result of energy dissipation	In air/water with gear disconnected
Transmission damping, C_{trans}	It is mainly due to friction in the gear system and frictional losses of the generator as frictional bearing losses	In water with transmission connected and generator connected to the transmission (without electrical load)
Generator damping, C_{gen}	It is by the generator armature (internal) resistance R_{arm}	It is due to the generator armature internal resistance R_{arm}, which is a function of the load resistance
Harness damping, C_{harn}	It is due to the load resistance RL used to harness energy	It is obtained by the performing a free decay test of the corresponding system

Analytical estimation of C_{total} is not possible, and hence, it is measured experimentally; there are four sources as summarized in Table 3.

The cylinder is initially displaced to undergo damped up and down movements with y_n and $y_{(n+1)}$ as any two consecutive peaks that are given as:

$$\frac{y_n}{y_{n+1}} = e^{(\zeta \omega_d T_d)} \tag{11}$$

where $T_d = \frac{2\pi}{\omega_d}$ and damping ratio $= \frac{1}{2\pi} \ln \frac{y_n}{y_{n+1}}$.

The open voltage across the generator is given by:

$$E = \alpha \frac{y(t)}{r_1} \tag{12}$$

The power harnessed by the load resistor R_L:

$$P_L = e_L I_{\text{arm}} = I_{\text{arm}}^2 R_L = \left[\frac{\frac{\dot{y}(t)}{r_1}\alpha}{R_{\text{arm}} + R_L} \right] R_L \tag{13}$$

4 Measurements and Data Analysis

In the measurement and data analysis of the *VIV* phenomenon, cylinder vertical displacement, water velocity, voltage generation at R_L, and the harnessed power

Table 4 Various input parameters that have significant effects on *VIVACE*

Parameter	Effect
Low damping	Enhanced synchronization range and *VIV* amplitude
R_L as infinity	Zero power take-off due to open ends
High damping	*VIV* amplitude and synchronization remains high
High Re values	Supports high oscillation amplitudes

are few important output parameters and those should be recorded during the experimental run. A rigorous evaluation of design, fabrication, and compatibility of various parts must be done via damping tests so that all parts of the *VIVACE* work properly at minimum friction. The role of free surface and bottom effects should be studied. Fourier spectral analysis is not applicable here; *VIV* time series are of nonlinear, non-stationary nature. So, Hilbert-Huang Transform (*HHT*) is used to analyze the resulted time series over large range of velocities and load resistor R_{load}. In the experimental runs, generated voltage and harnessed power can be studied at different velocities and R_{load}. Subsequently, η_{peak}, $\eta_{VIVACE,}$ and $\eta_{UL\text{-}VIVACE}$ can be calculated for the overall rating of the *VIVACE* device.

A basic parametric analysis to see the effect of various parameters is recorded in terms of dimensionless amplitude of *VIV,* power output, various efficiencies, etc. which suggests many important interrelationships are obtained that are summarized in the Table 4.

5 Conclusions and Future Scopes

Vortex-induced vibrations (*VIV)* have been studied and exploited for low damping only, and it is the first time that an ocean energy convertor has been devised to harness electricity with *VIV* under high damping. The vortex shedding phenomenon is mainly studied in low Reynolds number but in real ocean current flows at high Re. At higher Re, the amplitude of *VIV* increases which supports higher voltage generation. This review paper is aimed to put together the fundamentals of *VIVACE* device via hydrodynamic and mathematical models. The ocean energy convertors like turbines and watermills are unable to work at low water flow speeds, while *VIVACE* has ability to harness energy even in such low velocities at reasonably high efficiencies. In the future scope, the effect of high damping and high *Re* on wake characteristics and energy harvesting can be investigated. The optimum value of cylinder diameter and spring stiffness at given mass ratio can predicted to get a economic *VIVACE* device.

References

1. Bernitsas MM, Raghavan K (2004) Converter of current/tide/wave energy, provisional patent application, US Patent and Trademark Office Serial No. 60/628,252
2. Bernitsas MM, Raghavan K (2005) Supplement to the U.S. provisional patent application titled, converter of current, tide, or wave energy, University of Michigan Ref. No. 2973
3. Bernitsas MM, Raghavan K (2005) Fluid motion energy converter, U.S. Patent Application, United States Patent and Trademark Office, Serial No. 11/272,504
4. Bernitsas MM, Raghavan K (2005) Fluid motion energy converter, international provisional patent application, USA Patent and Trademark Office
5. Bernitsas MM, Ben-Simon Y, Raghavan K, Garcia EMH (2006) The VIVACE converter: model tests at high damping and reynolds number around 10^5. In: 25th international OMAE conference
6. Ogata K (2004) System dynamics, 4th edn. Prentice Hall, New Jersey
7. Szepessy S (1993) On the control of circular, cylinder flow by end plates. Euro J Mech B Fluids 12:217–244
8. Chen SS (1987) Flow-induced vibration of circular cylinder structures. Hemisphere Publishing Corporation, Springer, Washington
9. Khalak A, Williamson CHK (1999) Motions, forces and mode transitions in vortex-induced vibrations at low mass-damping. J Fluids Struct 13:813–851
10. Govardhan R, Williamson CHK (2000) Modes of vortex formation and frequency response of a freely vibrating cylinder. J Fluid Mech 420:85–130
11. Rood EP (1995) Free surface vorticity (Chap. 17). In: Green S (ed) Free-surface vorticity. Kluwer
12. Sarpkaya T (2000) A critical review of the intrinsic nature of vortex induced vibrations. J Fluids Struct 19(4):389–447
13. Walker DT, Lyzenga DR, Ericson EA, Lund DE (1996) Radar backscatter and surface roughness measurements for stationary breaking waves. Proc Roy Soc Lond A 452:1953–1984
14. Huang NE, Shen Z, Long SR, Wu MC, Shih HH, Zheng Q, Yen NC, Tung CC, Liu HH (1998) The empirical mode decomposition and the Hilbert spectrum for nonlinear and nonstationary time series analysis. Proc Roy Soc Lond A 454:903–995